



**HAL**  
open science

## **HARD QUARK-QUARK SCATTERING WITH EXCLUSIVE REACTIONS**

D. Barton, G. Bunce, A. Carroll, Y. Makdisi, B. Baller, G. Blazey, H. Courant, K. Heller, S. Heppelmann, M. Marshak, et al.

► **To cite this version:**

D. Barton, G. Bunce, A. Carroll, Y. Makdisi, B. Baller, et al.. HARD QUARK-QUARK SCATTERING WITH EXCLUSIVE REACTIONS. Journal de Physique Colloques, 1985, 46 (C2), pp.C2-115-C2-120. <10.1051/jphyscol:1985211>. <jpa-00224522>

**HAL Id: jpa-00224522**

**<https://hal.science/jpa-00224522v1>**

Submitted on 4 Feb 2008

**HAL** is a multi-disciplinary open access archive for the deposit and dissemination of scientific research documents, whether they are published or not. The documents may come from teaching and research institutions in France or abroad, or from public or private research centers.

L'archive ouverte pluridisciplinaire **HAL**, est destinée au dépôt et à la diffusion de documents scientifiques de niveau recherche, publiés ou non, émanant des établissements d'enseignement et de recherche français ou étrangers, des laboratoires publics ou privés.



HAL Authorization

## HARD QUARK-QUARK SCATTERING WITH EXCLUSIVE REACTIONS\*

D.S. Barton, G.M. Bunce, A.S. Carroll, Y.I. Makdisi, B. Baller\*, G.C. Blazey\*, H. Courant\*, K.J. Heller\*, S. Heppelmann\*, M.L. Marshak\*, E.A. Peterson\*, M.A. Shupe\*, D.S. Wahl\*, S. Gushue\*\* and J.J. Russell\*\*

*Brookhaven National Laboratory, Upton, New York 11973, U.S.A.*

*\*University of Minnesota, Minneapolis, Minnesota 55455, U.S.A*

*\*\*Southeastern Massachusetts University, North Dartmouth, Massachusetts 02747, U.S.A.*

Résumé - Nous présentons les résultats pour les réactions  $\pi^- p \rightarrow \pi^- p$  et  $\pi^- p \rightarrow \rho^- p$  à  $\theta_{c.m.} = 90^\circ$  ou  $-t = 9 \text{ GeV}^2/c^2$ . On observe un important signal  $\rho^- p$  et le  $\rho^-$  est fortement polarisé. Cette polarisation teste la prédiction de QCD selon laquelle les quarks ne peuvent pas renverser l'hélicité. Ce test est extrêmement mauvais.

Abstract - We present data from  $\pi^- p \rightarrow$  elastic and  $\rho^- p$  final states for scattering at  $90^\circ$  center of mass,  $-t = 9 \text{ GeV}^2/c^2$ . A large  $\rho^- p$  signal is seen and the  $\rho^-$  are strongly polarized. This polarization tests a QCD prediction that quarks cannot flip helicity. The test fails dramatically.

Exclusive two-body to two-body scattering at large momentum transfer represents a new laboratory for the study of hard scattering processes.<sup>1</sup> In general, several types of quark diagrams may contribute, as shown in Fig. 1 for meson-baryon scattering. Elastic scattering may proceed via any or all of the graphs, as can  $\pi^- p \rightarrow \rho^- p$ . A reaction such as  $\pi^- p \rightarrow K^0 \Lambda$  cannot occur via pure gluon exchange or quark interchange. There are a large number of two-body exclusive reactions experimentally accessible with  $\pi^\pm$  and  $K^\pm$  meson beams, and each is sensitive to different mixtures of the graphs shown in Fig. 1. If the quark graphs are flavor-independent, as expected for hard scattering where the asymptotic quark masses are small on the scale of the momentum transferred in the interaction, the amplitudes for each of the two-body exclusive reactions can be written in terms of the same quark scattering amplitudes, with corresponding relationships expected between the reaction cross sections.

In addition, for many possible two-body exclusive reactions polarization may be measured for a final state particle through its decay, and this can further constrain the quark amplitudes. For example, we report here on the reaction  $\pi^- p \rightarrow \rho^- p$  where the angular distribution of the  $\pi^-$  from the  $\rho^- \rightarrow \pi^- \pi^0$  decay analyzes the helicity state of the  $\rho^-$ . If the pure gluon exchange graph (Fig. 1a) were to dominate this reaction, helicity conservation at the quark level, a prediction of quantum chromodynamics, would require that the  $\rho^-$  helicity be the same as that of the incident  $\pi^-$ , or zero. Helicity-flip amplitudes are expected to be suppressed by a factor  $m_q/\sqrt{s} \sim 10^{-3}$  for our case where  $\sqrt{s} \sim 2 \text{ GeV}$  and we assume the asymptotically free quark mass of about 5 MeV. The other graphs, quark annihilation and interchange, can give a  $\rho^-$  with helicity  $\pm 1$ .

The momentum transfer above which one can successfully apply perturbative QCD is debatable.<sup>2</sup> However, many experimental phenomena indicate that an asymptotic region sets in for  $p_T > 1.5 \text{ GeV}/c$  or  $t > 5 \text{ GeV}^2/c^2$ . Examples are the  $Q^2$  dependence of the proton form factor (constant for  $Q^2 > 5$ ),<sup>3</sup> that fixed angle elastic scattering follows dimensional counting predictions for  $-t > 5 \text{ GeV}^2/c^2$ ,<sup>4</sup> and that elastic cross

\*Work performed under the auspices of the U.S. Department of Energy and the National Science Foundation.

sections develop a flat central region at this value of momentum transfer.<sup>5</sup> For this experiment,  $-t = 9 \text{ GeV}^2/c^2$ . Exclusive cross sections may be calculable with perturbative QCD, but the calculation requires knowledge of the wave functions and each quark must be accounted for. Farrar has developed a computer code to calculate cross sections for such reactions.<sup>6</sup> In addition, there are other theoretical models for exclusive scattering.<sup>7</sup>

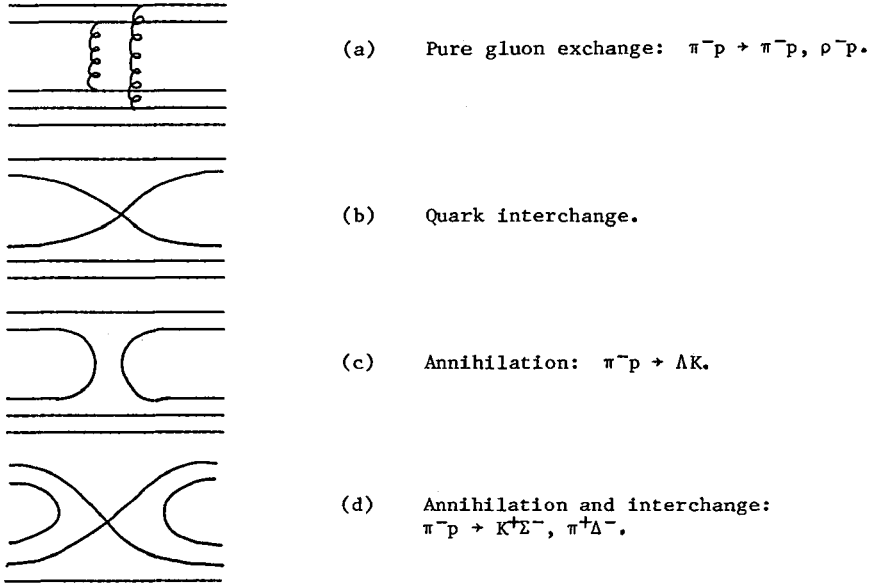


Fig. 1. Quark diagrams for meson-baryon exclusive scattering. Example reactions for the diagram are shown. The reactions listed in (a) can proceed via diagrams (b), (c), (d). Similarly,  $\pi^-p \rightarrow \Lambda K$  can proceed via (d).

We report on an experiment performed at the Brookhaven AGS with an intense 10 GeV/c  $\pi^-$  beam incident on a hydrogen target. The first results, on elastic scattering and on the  $\rho^-p$  final state, will be presented. The apparatus (Fig. 2) consisted of a single arm magnetic spectrometer which selected events with a positive particle with momentum greater than 5 GeV/c at  $22^\circ$  in the laboratory or near  $90^\circ$  in the  $\pi^-p$  elastic center of mass system. A large-aperture array of three proportional wire chambers recorded track information on the opposite side. With an event trigger for  $\pi^-p \rightarrow$  positive + X, and  $P_T > 1.9 \text{ GeV}/c$ , events were collected simultaneously for  $\pi^-p, \rho^-p, K^+\Sigma^-, \pi^+\Delta^-$ , and other exclusive final states. For elastic scattering at  $90^\circ$ ,  $P_T = 2.1 \text{ GeV}/c$ .

The spectrometer arm was located in a building which could pivot about the center of the target to select the scattering angle  $\theta$ . The analyzing magnet was placed on its side so that its gap of 18" defined a small range of laboratory angles,  $\Delta\theta = \pm 2.5^\circ$ . The magnet deflected positives down with a transverse kick of 0.8 GeV/c. The vertical deflection decoupled the momentum measurement from the large horizontal projection of the 1 meter long target at  $\theta = 22^\circ$ . Assuming a point target, a momentum could be determined using a matrix trigger between drift cells in DWC1 and DWC2 after the magnet. We also required a matrix trigger between scintillator hodoscope elements in HODO 2 and HODO 3, which reduced accidental triggers. All detectors downstream of the magnet were mounted on a table which was tilted  $8.1^\circ$  to match the central momentum for elastic scattering. Two threshold Cerenkov counters on the tilt table, one with  $\gamma_{\text{threshold}} = 21.5$ , the other with  $\gamma_{\text{threshold}} = 9.6$ , were used to

distinguish between pions, kaons, and protons in the spectrometer arm. The momentum resolution of the arm, with proportional wire chambers upstream and narrow-cell drift chambers downstream was  $\Delta p/p = 0.5\%$  at 5 GeV/c.

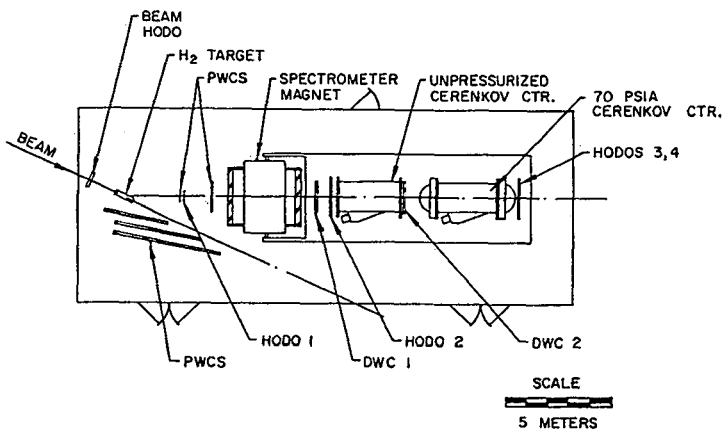


Fig. 2. Plan view of experimental apparatus for measuring exclusive reactions.

$5 \times 10^6$  events were recorded for  $5 \times 10^{12}$  incident pions on target. Most triggers were caused by the more copious lower momentum particles which were either accepted by the trigger (there was some acceptance down to  $P_T = 1.4$  GeV/c), or which scattered from the magnet iron and fooled the trigger. Four percent of the events on tape had a single spectrometer track with  $P_T > 1.8$  GeV/c. Half the spectrometer tracks had no Cerenkov signal, indicating a spectrometer proton. Of these, 7% had a single side track which formed an acceptable vertex with the incident beam track and the track in the spectrometer arm. The momentum of each beam  $\pi^-$  was measured by bending the beam vertically upstream of the target, with scintillator hodoscope fingers in the beam to tag the particle position after the vertical deflection. We obtained  $\Delta p/p \approx 1\%$  (rms) for these data, which gave  $\Delta$  (missing mass) $^2 \approx .2$  GeV $^2/c^2$  for the reaction  $\pi^- p \rightarrow p + X$ .

We show in Fig. 3a the missing mass distribution for those with a proton in the spectrometer and a single track in the side array. The elastic sample, selected requiring coplanarity and opening angle cuts, is indicated by the shaded region. Our preliminary value for the elastic cross section at 10 GeV/c, 90° CMS,  $-t = 9$  GeV $^2/c^2$  is  $d\sigma/dt \approx .2$  nb/ GeV $^2/c^2$ , in reasonable agreement with previous work.<sup>3</sup> After removing elastics, the candidate  $\rho$  events appear as a shoulder in the .5 GeV $^2/c^2$  missing mass squared region. If we subtract the background from higher masses by assuming a power law dependence, we obtain the distribution shown in Fig. 3b for the reaction  $\pi^- p \rightarrow p\rho^-$ ,  $\rho^- \rightarrow \pi^- \pi^0$ . The apparent width of the  $\rho$  mass is comparable with the resolution, as seen in the elastic sample. The ratio of cross sections is approximately  $\rho^- p/\text{elastic} \approx 1.0$ .

The angular distribution of the  $\pi^-$  from  $\rho^-$  decay analyzes the helicity of the  $\rho^-$ . In the Gottfried-Jackson frame, after eliminating parity violating terms, the distribution of the  $\pi^-$  is given by<sup>8</sup>

$$W(\theta, \phi) \approx \frac{3}{4\pi} [\rho_{00} \cos^2 \theta + (\rho_{11} - \rho_{1-1}) \sin^2 \theta \cos^2 \phi + (\rho_{11} + \rho_{1-1}) \sin^2 \theta \sin^2 \phi - 2\rho_{10} \sin 2\theta \cos \phi] \quad (1)$$

where  $\theta$  is the polar angle from the incident  $\pi^-$  direction in the  $\rho^-$  center of mass frame and  $\phi$  is the azimuthal angle.  $\rho_{ij}$  is a spin-density matrix element for helicity  $i$ ,  $j$   $\rho^-$  amplitudes. A non-resonant S-wave  $\pi^- \pi^0$  background would have an isotropic angular distribution.

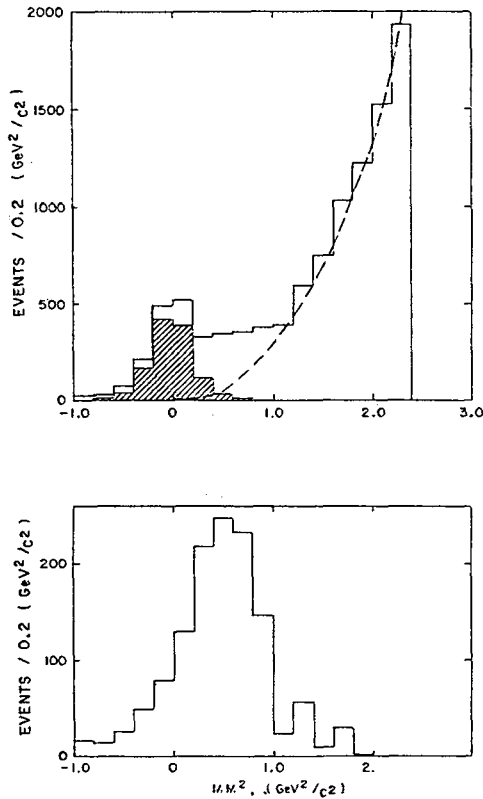


Fig. 3a. Missing mass squared distribution for the reaction  $\pi^- p + pX$  near  $\theta=90^\circ$  cm with a single track in the side array. The shaded region represents events whose angular correlations satisfy elastic kinematics. Figure 3b. is the distribution resulting from subtraction of both the elastic events and the power law fit shown by the dashed curve in Fig. 3a.

In Fig. 4a and 4b we show the projections of the angular distribution of events within a  $\rho$ -cut ( $0.2 < MM^2 < 0.8 \text{ GeV}^2$ ), plotting events versus  $\phi$  and  $\cos \theta$ . There are two regions where the acceptance is poor--a small region near  $\cos \theta = -1$  where the elastic candidates have been eliminated and near  $\cos \theta = +1$ ,  $\phi = 0^\circ$  where backward decays toward the beam line miss our side chambers. The data in Fig. 4a show qualitatively the two lobes of the  $\sin^2 \theta \sin^2 \phi$  distribution, indicating the presence of helicity  $\pm 1$ . The  $\cos \theta$  distribution in Fig. 4b shows no indication of a  $\cos^2 \theta$  contribution of the form indicated by the  $\Delta$ s. In both the  $\phi$  and  $\cos \theta$  projections we have indicated a Monte Carlo acceptance corrected distribution of  $1/3 \sin^2 \theta \sin^2 \phi + 2/3$  isotropic which provides a good qualitative fit. A Monte Carlo simulation for an isotropic decay, which indicates acceptance effects and the effect of any s-wave background contribution, follows the data closely in the  $\cos \theta$  projection and is flat in the  $\phi$  projection.

Referring to the angular distribution, equation (1), the matrix element  $\rho_{1-1}$  must be large to obtain a  $\sin^2 \theta \sin^2 \phi$  distribution. Our data rule out a  $\cos^2 \theta$  distribution quite strongly. The  $\rho_{1-1}$  term requires that a fixed initial  $\pi^- p$  helicity state can go to both helicity  $\pm 1$  final states of the  $\rho^-$ . For example, an initial state with target proton helicity  $+1/2$  can go to a helicity  $-1 \rho^-$ . This cannot happen without flipping a quark helicity. Thus, the data show that quark helicities are not con-

served, which is in clear violation of QCD. (The model of ref. 7, however, does allow for and predict a  $\sin^2\theta \sin^2\phi$  dependence--see Preparata, this conference.)

The large  $\rho^-p$  signal, roughly equal to the elastic cross section, is also surprising. We have looked for one other two-body reaction,  $\pi^-p \rightarrow K\Lambda$ , and we see one possible event versus  $\sim 1000$  elastics and  $\rho^-p$ . If all quark scattering amplitudes were equal at  $90^\circ$ , one would expect roughly equal cross sections for two body scattering, independent of quark flavor.<sup>9</sup> Thus, there appear to be strong dynamical effects at work here. We have a large amount of data still to analyze, which includes both positive and negative beam runs. Accessible reactions include  $\pi^-p \rightarrow K^+\Sigma^-$ ,  $K^+\Sigma^*$ ,  $\pi^+\Delta^-$ ;  $K^-p$  and  $K^+p$  elastic;  $\pi^+p \rightarrow \rho^+p$ ,  $K^+\Sigma^+$ .

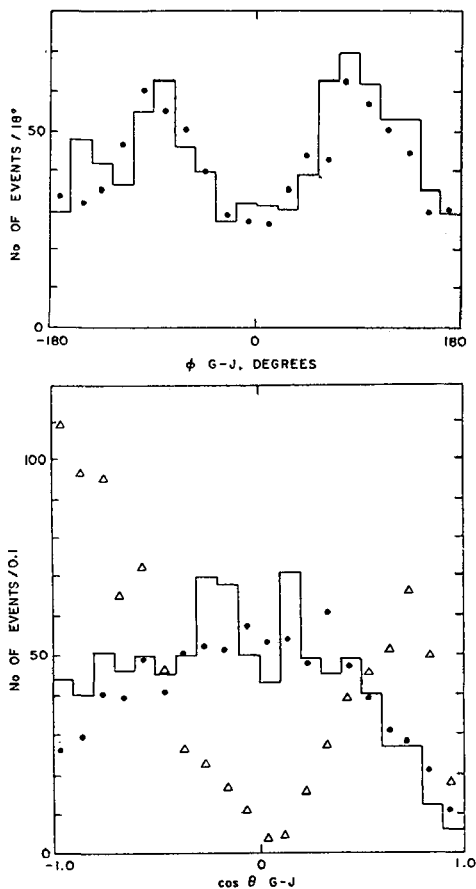


Fig. 4. The  $\pi^-$  distribution from the  $\rho^-$  decay in the Gottfried-Jackson frame. Both  $\phi$  (a) and  $\cos \theta$  (b) distributions are fit with the combination  $1/3 \sin^2\theta \sin^2\phi + 2/3$  isotropic indicated by the dots. In Fig. 4b, the normalized distribution  $\cos^2\theta$  is indicated by the  $\Delta$ 's.

#### Acknowledgements

We are pleased to acknowledge the technical support of E. Bihn, G. Grego, S. Marino and many members of the MPS Group at Brookhaven. Many members of the EP&S Division provided vital assistance in the design and construction of the experiment, particularly J. Walker and J. Mills. J. Steinbeck made important contributions. F. Paige, L. Trueman, G. Farrar and J. Soffer aided in the understanding of our results.

References

1. See P. Grannis, "Workshop on the AGS Fixed Target Program," BNL (1978).
2. G.R. Farrar, Phys. Rev. Letters 53, 28 (1984); N. Isgur and C. Smith, Phys. Rev. Letters 52, 1080 (1984).
3. M.D. Mestayer, SLAC Report No. 214 (1978), unpublished.
4. S.J. Brodsky and G.R. Farrar, Phys. Rev. D11, 1309 (1975).
5. C. Baglin, et al., Nucl. Phys. B98, 365 (1975); K.A. Jenkins, et al., Phys. Rev. D21, 2445 (1980).
6. G.R. Farrar, Proc. of the Third LAMPF II Workshop, edited by J.C. Allred, et al., 562 (1983). For a discussion of exclusives and QCD, see G.P. Lepage and S.J. Brodsky, Phys. Rev. D22, 2157 (1980).
7. The Massive Quark Model, which treats effects of confinement dynamics, is discussed in a series of papers. See P. Chiappetta and J. Soffer, Phys. Rev. D28, 2162 (1983); G. Preparata and J. Soffer, Phys. Lett. 93B, 187 (1980) and Phys. Lett. 86B, 304 (1979).
8. J.D. Jackson, High Energy Physics Proc. Les Houches Summer School, 1965, editors C. DeWitt and M. Jacob (eqn. 3.18); K. Gottfried and J.D. Jackson, Nuovo Cimento 33, 309 (1964); S. Gasiorowicz, Elementary Particle Physics, p. 459, Wiley and Sons (1967).
9. P. Fishbane and C. Quigg, Nucl. Phys. B61, 469 (1979).